



Kinetics and mechanism of 2,6-dimethyl-aniline degradation by hydroxyl radicals

Nonglak Boonrattanakij^{a,b}, Ming-Chun Lu^c, Jin Anotai^{d,*}

^a International Postgraduate Programs in Environmental Management, Graduate School, Chulalongkorn University, Bangkok 10330, Thailand

^b National Center of Excellence for Environmental and Hazardous Waste Management (NCE-EHWM), Chulalongkorn University, Bangkok 10330, Thailand

^c Department of Environmental Resources Management, Chia-Nan University of Pharmacy and Sciences, Tainan 717, Taiwan

^d National Center of Excellence for Environmental and Hazardous Waste Management Department of Environmental Engineering, Faculty of Engineering, King Mongkut's University of Technology Thonburi, Bangkok 10140, Thailand

ARTICLE INFO

Article history:

Received 27 May 2009

Received in revised form 20 July 2009

Accepted 21 July 2009

Available online 28 July 2009

Keywords:

Advanced oxidation processes

Fenton process

2,6-Dimethyl-aniline

Hydroxyl radicals

Kinetics

ABSTRACT

This research investigated the intrinsic second-order rate constant between 2,6-dimethyl-aniline (2,6-DMA) and hydroxyl radicals (OH[•]) using Fenton's reactions under both batch and continuous operations. The competitive kinetics technique with aniline as a reference compound was employed. In the batch study under various conditions, the second-order rate constants of 2,6-DMA with OH[•] were between 1.59×10^{10} and $1.80 \times 10^{10} \text{ M}^{-1} \text{ s}^{-1}$ with a mean of $1.71 \times 10^{10} \text{ M}^{-1} \text{ s}^{-1}$ which equals the average value obtained from the continuous study as well. The concentrations of OH[•] at the steady state under the continuous mode were estimated to be between 4.85×10^{-10} and $6.82 \times 10^{-10} \text{ mM}$. 2,6-dimethyl-nitrobenzene, 2,6-dimethyl-phenol, 2,6-dimethyl-nitrophenol, 2,6-dimethyl-hydroquinone, 2,6-dimethyl-*p*-benzoquinone, and 2,6-dimethyl-3-hydroxy-*p*-benzoquinone were identified as the aromatic by-products indicating that the methyl group on the aromatic ring was not susceptible to OH[•] attack. Maleic, lactic, oxalic, acetic, and formic acids were found as generated carboxylic acids. An oxidation pathway of 2,6-DMA by OH[•] is also proposed.

© 2009 Elsevier B.V. All rights reserved.

1. Introduction

There are several hazardous chemicals that are environmentally persistent and cannot be degraded by traditional treatment processes. 2,6-Dimethyl-aniline (2,6-DMA) has been used widely as a chemical intermediate to produce many products such as pesticides, dyestuffs, antioxidants, pharmaceuticals, and other products [1]. It is a metabolite of the xylidine group of anesthetics including lidocaine, and is produced by the reduction of certain azo dyes by intestinal microflora. It may also enter the environment through degradation of certain pesticides. Wastewaters contaminated with 2,6-DMA from these manufacturers can pose adverse impacts on receiving waters due to its biorefractory and highly toxic properties. This chemical has also been classified by the International Agency for Research on Cancer (IARC) as a group 2B carcinogen [2]. As a result, appropriate and effective treatment technologies are needed to purify or clean up these contaminated wastewaters.

Advanced oxidation processes (AOPs) are a possible alternative that can provide the destruction of refractory and hazardous organic compounds. Hydroxyl radicals (OH[•]) generated in the AOPs are extremely reactive, short lived, and unselective transient species that can readily oxidize organic/inorganic pollutants in water and wastewater and convert them into simple, relatively harmless substances. A number of methods can lead to the generation of OH[•] including H₂O₂/UV, O₃/H₂O₂, O₃/UV, TiO₂/UV, and Fenton's family, which is of interest in this research. The Fenton process is normally initiated by the addition of ferrous (Fe²⁺) and hydrogen peroxide (H₂O₂), known as "Fenton's reagent". The conventional Fenton process is simple, effective, and requires no high capital investment. Therefore, it was selected as a means for OH[•] generation in this study.

Although the oxidation of 2,6-DMA by OH[•] has been investigated previously by Ting et al. [3], no intrinsic rate constant of the reaction between 2,6-DMA and OH[•] has been reported. This constant is very important and can provide useful scientific information. As a result, this research focused on the determination of the second-order rate constant between 2,6-DMA and OH[•] using a competitive kinetics technique. This technique has been used successfully by Shen et al. [4] to determine the reaction rate constant between *p*-chloronitrobenzene and ozone using nitrobenzene and chlorobenzene as reference compounds. In

* Corresponding author. Tel.: +66 2 470 9166; fax: +66 2 470 9165.
E-mail address: jin.ano@kmutt.ac.th (J. Anotai).

addition, the degradation pathway of 2,6-DMA by OH• oxidation was also explored.

2. Materials and methods

2.1. Chemicals and analytical method

All chemical substances used in the experiment including 2,6-DMA, *n,n*-dimethyl-aniline (*n,n*-DMA), aniline (AN), 2,6-dimethyl-phenol (2,6-DMP), 2,6-dimethyl-nitrobenzene (2,6-DMN), 2,6-dimethyl-benzoquinone (2,6-DMB), FeSO₄·7H₂O, and H₂O₂ were reagent grade with high purity. AN was used as a reference compound in the rate constant determination between 2,6-DMA and OH•. The accuracy of the competitive kinetics technique was verified using *n,n*-DMA as a pre-tested compound. Both compounds were selected because their molecular structures were quite similar to 2,6-DMA, which could be accurately quantified under the same GC conditions. Three compounds, 2,6-DMP, 2,6-DMN, and 2,6-DMB, were used to cross-check the identification of oxidation intermediates from 2,6-DMA oxidation by OH•. Deionized water from a Millipore system with a resistivity of 18.2 MΩ cm⁻¹ was used to prepare all solutions.

The samples taken at selected time intervals were immediately injected into tubes containing sodium hydroxide solution to stop further reaction and were then filtered through 0.22 μm syringe micro-filters to separate precipitated iron from the solution. Subsequently, the residual organic compounds were quantified by Shimadzu GC-17A gas chromatograph equipped with a flame ionization detector and Hewlett-Packard HP-5 capillary column (0.53 mm × 15 m length). Exactly 1.0 μL of samples was injected into the injection port. The column temperature was initially set at 85 °C for 3 min, then increased by 65 °C min⁻¹ to 200 °C and maintained at this temperature for the final 5 min. Injector and detector temperatures were set at 250 °C.

Identification of organic intermediates from the Fenton's reaction was determined by injecting 1.0 μL of the extraction solvent into the Agilent Technologies 6890N Network GC System equipped with a J&W DB-5MS capillary column (0.25 mm × 30 m) and connected with the 5973 Network Mass Selective Detector. The GC temperature program was as follows: 40 °C for 2 min, followed by a 15 °C min⁻¹ ramp to 280 °C, then hold for 5 min. Carboxylic acids were determined by Ion Chromatograph (Shimadzu) equipped with a SCL-10A VP system controller, DGU-20A₃ degasser, LC-20AD VP liquid chromatograph, CTO-20A column oven, CDD-10A VP conductivity detector, Shim-pack IC-GA3 guard column, and Shim-pack IC-A3 analytical column (4.6 mm × 15 cm). The mobile phase was 8.0 mM *p*-hydroxybenzoic acid and 3.2 mM bis(2-hydroxyethyl)iminotris(hydroxymethyl)methane. The flow rate and temperature were set at 1.2 mL min⁻¹ and 40 °C, respectively. The injecting sample volume was 10 μL. Total organic carbon (TOC) content was measured by Shimadzu TOC-V_{CPN}. Ferrous was determined by light absorbance measurement at 510 nm after being complexed with 1,10-phenanthroline using a UV-vis spectrophotometer [5]. Residual H₂O₂ was analyzed by an iodometric titration with Na₂S₂O₃ solution [6].

2.2. Fenton experiment

2.2.1. Batch study

The synthetic wastewater was prepared by dissolving appropriate amounts of organic(s) with deionized water. A predetermined amount of FeSO₄·7H₂O was added as the source of Fe²⁺. Then, the stirrer was used to mix the solution and the pH was adjusted to 3.0 ± 0.05 by 1:4 H₂SO₄. Hydrogen peroxide solution was finally added and the reaction was simultaneously started. Solution pH

was controlled constantly by the addition of H₂SO₄ or NaOH whenever necessary, while the temperature was maintained at 25 ± 0.2 °C.

2.2.2. Continuous study

Synthetic wastewater with Fe²⁺ dissolution and hydrogen peroxide solution were separately, but continuously, fed into a 0.5 L beaker. Solution pH was controlled constantly by the addition of H₂SO₄ or NaOH whenever necessary. Temperature was controlled at 25 ± 0.2 °C throughout the experiment. The sample was taken every 30 min and was analyzed for its composition until reaching the steady state.

3. Results and discussion

3.1. Experimental controls

This portion of the experiment was to determine the direct oxidation of 2,6-DMA, *n,n*-DMA, and AN by H₂O₂ as well as their volatilization. The results demonstrated that these three compounds could not be effectively oxidized by H₂O₂ or significantly volatilized to the atmosphere during the experimental period. The disappearance from both effects was less than 5% in all cases. As a result, it confirms that these compounds could be degraded effectively under the studied conditions only in the presence of OH•.

3.2. Validation of competitive technique

It is important to verify the competitive kinetics technique as well as the value of the rate constant between the reference compound (AN) and OH•, which was obtained from another study. It is well known that OH• will react with organics following the second-order rate law with respect to organic and OH• concentrations. This can generally be expressed for a batch reactor as:

$$\frac{d[\text{organic}]}{dt} = -k_{\text{OH}\cdot, \text{org}}[\text{organic}][\text{OH}\cdot] \quad (1)$$

When two organics are present together in the OH• oxidation system, they will competitively react with OH•. The reaction rate equations for both organics can be written as in Eqs. (2) and (3) and can be further derived in a competition reaction manner as follows:

$$\frac{d[\text{org}_1]}{dt} = -k_{\text{org}_1}[\text{org}_1][\text{OH}\cdot] \quad (2)$$

$$\frac{d[\text{org}_2]}{dt} = -k_{\text{org}_2}[\text{org}_2][\text{OH}\cdot] \quad (3)$$

$$\frac{\text{Eq. (2)}}{\text{Eq. (3)}} = \frac{d[\text{org}_1]/dt}{d[\text{org}_2]/dt} = \frac{-k_{\text{org}_1}[\text{org}_1][\text{OH}\cdot]}{-k_{\text{org}_2}[\text{org}_2][\text{OH}\cdot]} \quad (4)$$

$$\frac{(1/[\text{org}_1])(d[\text{org}_1]/dt)}{(1/[\text{org}_2])(d[\text{org}_2]/dt)} = \frac{k_{\text{org}_1}}{k_{\text{org}_2}} \quad (5)$$

$$\frac{\int_0^t \frac{1}{[\text{org}_1]} \frac{d[\text{org}_1]}{dt} dt}{\int_0^t \frac{1}{[\text{org}_2]} \frac{d[\text{org}_2]}{dt} dt} = \frac{k_{\text{org}_1}}{k_{\text{org}_2}} \quad (6)$$

$$\frac{\ln([\text{org}_1]_t/[\text{org}_1]_0)}{\ln([\text{org}_2]_t/[\text{org}_2]_0)} = \frac{k_{\text{org}_1}}{k_{\text{org}_2}} \quad (7)$$

$$\ln \left(\frac{[\text{org}_1]_t}{[\text{org}_1]_0} \right) = \frac{k_{\text{org}_1}}{k_{\text{org}_2}} \ln \left(\frac{[\text{org}_2]_t}{[\text{org}_2]_0} \right) \quad (8)$$

where [org₁]₀, [org₁]_t, and [org₂]₀, [org₂]_t are the concentrations of org₁ and org₂ at the beginning and specific time, respectively; [OH•]

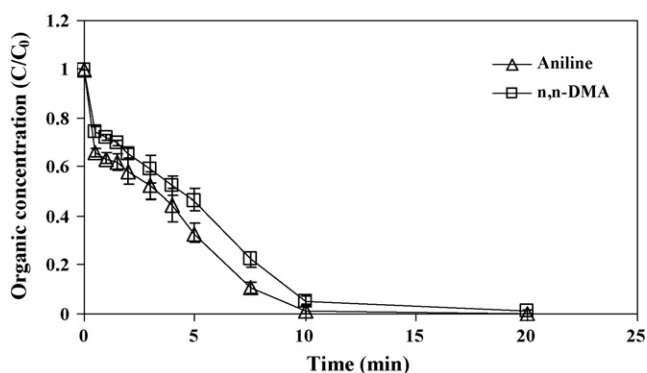


Fig. 1. Average degradation profiles of AN and *n,n*-DMA with their maximum and minimum bars from triplicate runs under a batch operation: [AN] = 1 mM, [*n,n*-DMA] = 1 mM, [Fe²⁺] = 1 mM, [H₂O₂] = 20 mM, at pH 3 and 25 °C.

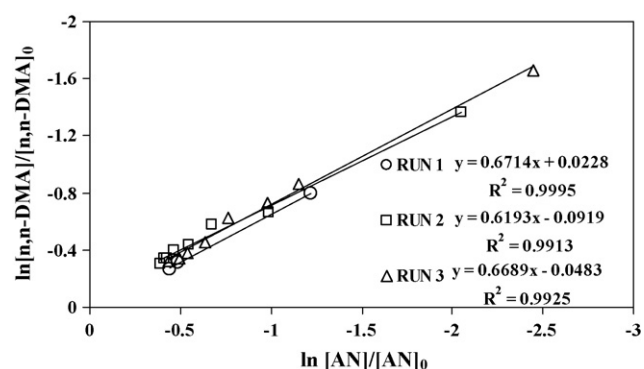


Fig. 2. Determination of the rate constant for the reaction between *n,n*-DMA & AN and OH[•] by Fenton's reaction under a batch operation: [AN] = 1 mM, [*n,n*-DMA] = 1 mM, [Fe²⁺] = 1 mM, [H₂O₂] = 20 mM, at pH 3 and 25 °C.

is the concentration of OH[•]; k_{org1} and k_{org2} are the rate constants of OH[•] reacting with org₁ and org₂, respectively. A preliminary study was conducted to verify the accuracy of this competitive kinetics technique by monitoring the degradation of AN with the OH[•] rate constant of $4.8 \times 10^9 \text{ M}^{-1} \text{ s}^{-1}$ [7] by Fenton process in the presence of *n,n*-DMA given its second-order rate constant with OH[•] of $2.9 \times 10^9 \text{ M}^{-1} \text{ s}^{-1}$ [7]. Hence, the theoretical ratio of the rate constants between *n,n*-DMA and AN is 0.60. Data repeatability and reliability were also checked as shown in Fig. 1 in which the experiments were done in triplicate. The results from Fig. 2, showing the plot between $\ln([n,n\text{-DMA}]/[n,n\text{-DMA}]_0)$ versus $\ln([AN]/[AN]_0)$, depicts a linear relationship with the slope representing the ratio

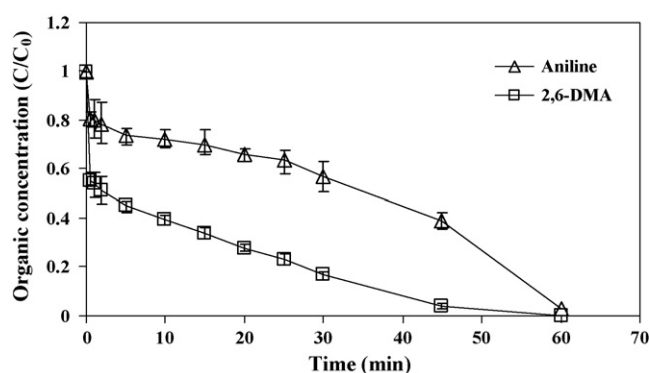


Fig. 3. Average degradation profiles of AN and 2,6-DMA with their maximum and minimum bars from triplicate runs under a batch operation: [AN] = 1 mM, [2,6-DMA] = 1 mM, [Fe²⁺] = 1 mM, [H₂O₂] = 20 mM, at pH 3 and 25 °C.

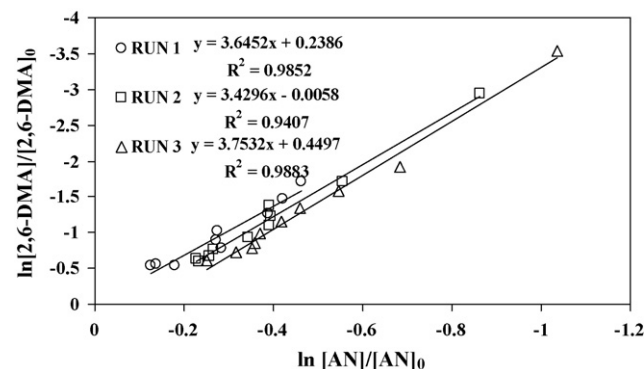


Fig. 4. Determination of the rate constant for the reaction between 2,6-DMA & AN and OH[•] by Fenton's reaction under a batch operation: [AN] = 1 mM, [2,6-DMA] = 1 mM, [Fe²⁺] = 1 mM, [H₂O₂] = 20 mM, at pH 3 and 25 °C.

of the rate constants between AN and *n,n*-DMA as stated in Eq. (8). An average slope of 0.65 was obtained, which was close to the theoretical value of 0.60; hence, this competition technique is valid.

3.3. Intrinsic rate constant of 2,6-dimethyl-aniline with hydroxyl radical

3.3.1. Batch study

In this section, the intrinsic rate constant of 2,6-DMA with OH[•] was determined in a batch reactor using AN as a reference compound following a similar procedure as in the previous experiment. Fig. 3 shows the time profiles of AN and 2,6-DMA and implies that OH[•] reacted with 2,6-DMA more selectively than AN. Moreover, it

Table 1
Second-order intrinsic rate constant between 2,6-DMA and OH[•].

Operation mode	Run number	2,6-DMA (mM)	AN (mM)	Fe ²⁺ (mM)	H ₂ O ₂ (mM)	k (M ⁻¹ s ⁻¹)
Batch	1	1	1	1	20	1.65×10^{10}
	2	1	1	1	20	1.75×10^{10}
	3	1	1	1	20	1.80×10^{10}
	4	0.5	1	1	20	1.73×10^{10}
	5	1	0.5	1	20	1.59×10^{10}
	6	0.5	0.5	1	20	1.59×10^{10}
	7	1	1	1.5	30	1.74×10^{10}
	8	1	1	2	40	1.77×10^{10}
	9	1	1	1	30	1.76×10^{10}
Continuous	10	1	1	1	20	1.70×10^{10}
	11	1	1	1	20	1.71×10^{10}
Average						1.71×10^{10}

was found that the ratios of the rate constant as represented by the slopes were quite steady with an average of 3.61 (Fig. 4). The rate constants obtained from various experimental conditions were found to be in between 1.59×10^{10} and $1.80 \times 10^{10} \text{ M}^{-1} \text{ s}^{-1}$ with an average of $1.71 \times 10^{10} \text{ M}^{-1} \text{ s}^{-1}$ as summarized in Table 1. This value is within the typical range of the rate constants for aromatic compounds with OH^\bullet of 10^9 to $10^{10} \text{ M}^{-1} \text{ s}^{-1}$ [8].

3.3.2. Continuous study

To verify the rate constant obtained from the previous section, a continuous study was also carried out. The reaction rate equations under a continuous operation could be derived as follows:

$$\frac{d[2,6\text{-DMA}]}{dt} = -k_{2,6\text{-DMA}}[2,6\text{-DMA}]_e[\text{OH}^\bullet] + Q([2,6\text{-DMA}]_i - [2,6\text{-DMA}]_e) \quad (9)$$

$$\frac{d[\text{AN}]}{dt} = -k_{\text{AN}}[\text{AN}]_e[\text{OH}^\bullet] + Q([\text{AN}]_i - [\text{AN}]_e) \quad (10)$$

At the steady state, $d[2,6\text{-DMA}]/dt$ and $d[\text{AN}]/dt = 0$

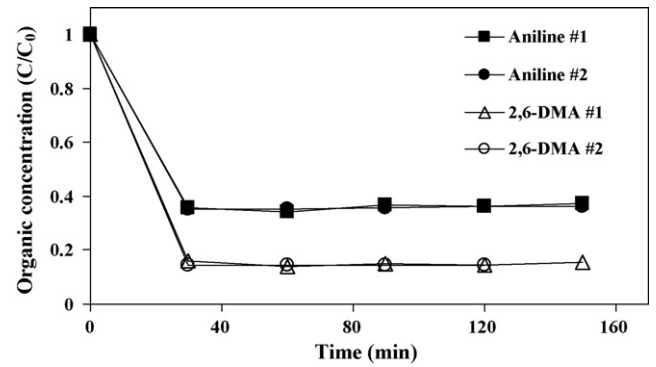


Fig. 5. Competition oxidation of AN and 2,6-DMA by Fenton's reaction under a continuous operation: $[\text{AN}] = 1 \text{ mM}$, $[2,6\text{-DMA}] = 1 \text{ mM}$, $[\text{Fe}^{2+}] = 1 \text{ mM}$, $[\text{H}_2\text{O}_2] = 20 \text{ mM}$, at pH 3 and 25°C .

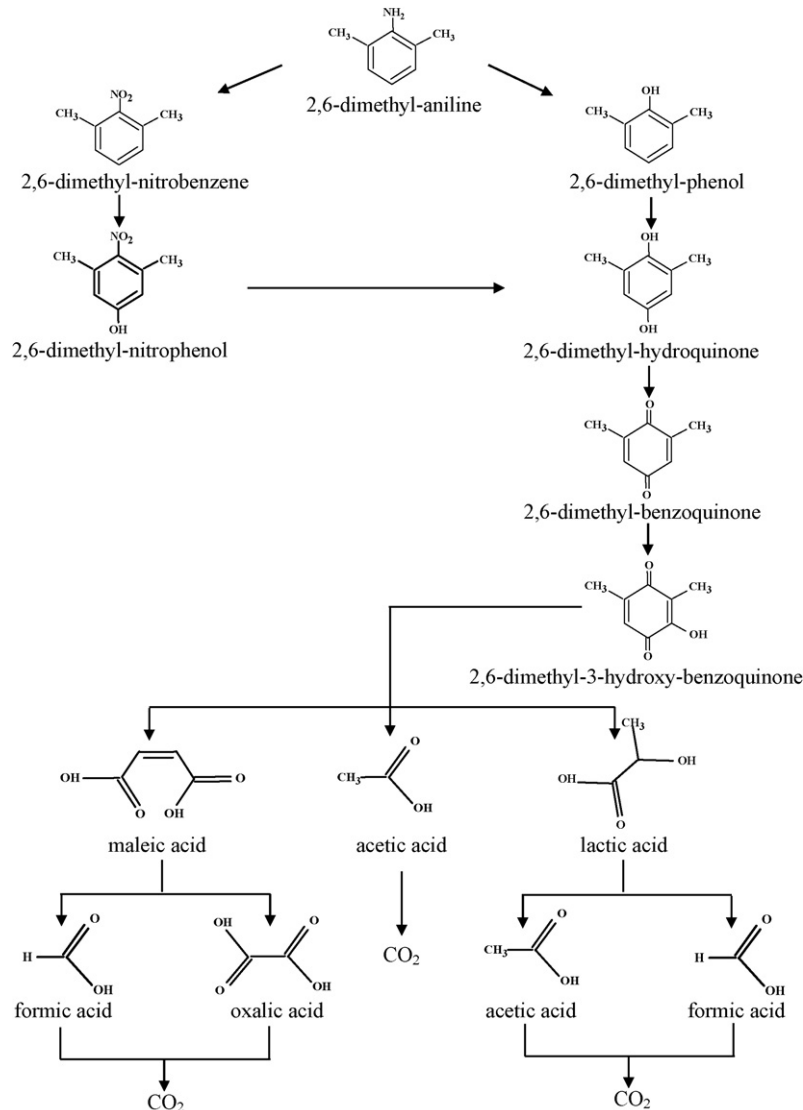


Fig. 6. Proposed reaction pathway for the mineralization of 2,6-DMA by OH^\bullet .

Hence, Eq. (9)/Eq. (10)

$$\frac{k_{2,6\text{-DMA}}[2,6\text{-DMA}]_e [\text{OH}^\bullet]}{k_{\text{AN}}[\text{AN}]_e [\text{OH}^\bullet]} = \frac{Q ([2,6\text{-DMA}]_i - [2,6\text{-DMA}]_e)}{Q ([\text{AN}]_i - [\text{AN}]_e)} \quad (11)$$

$$\frac{k_{2,6\text{-DMA}}}{k_{\text{AN}}} = \frac{([2,6\text{-DMA}]_i - [2,6\text{-DMA}]_e)}{([\text{AN}]_i - [\text{AN}]_e)} \frac{[\text{AN}]_e}{[2,6\text{-DMA}]_e} \quad (12)$$

where $[2,6\text{-DMA}]_i$, $[2,6\text{-DMA}]_e$ and $[\text{AN}]_i$, $[\text{AN}]_e$ are the concentrations of 2,6-DMA and AN in the influent and effluent, respectively, and Q is the total flow rate. Fig. 5 shows the results from co-oxidation of 2,6-DMA and AN by Fenton's reaction under a continuous feed mode. It can be seen from the figure that the data obtained from two different runs with similar conditions were very similar. Consequently, this verified the consistency of the experimental set up and procedure. The concentrations of AN and 2,6-DMA reached the steady state within 30 min. Fe^{2+} and H_2O_2 were also steady after 30 min (data not shown). The second-order intrinsic rate constant from this continuous experiment was determined by following Eq. (12) and found to be $1.71 \times 10^{10} \text{ M}^{-1} \text{ s}^{-1}$. This equals the average value obtained from the batch study. In addition, since the influent flow rates were also known, the concentrations of OH^\bullet at the steady state could be estimated and were found to be in the range of 4.85×10^{-10} to $6.82 \times 10^{-10} \text{ mM}$. Due to its high reactivity and short lifetime, the concentration of OH^\bullet in aqueous solution can be expected as very low depending on the presence of reactants, scavengers, organic compounds, and environmental conditions. This finding is consistent with several other studies. Lindsey and Tarr [8] quantified the OH^\bullet during Fenton oxidation of 0.2 mM of benzoic acid under a batch mode and found it to be within 1×10^{-8} to $1 \times 10^{-11} \text{ mM}$. Hoigne [9] found the steady state concentration of OH^\bullet to be a function of dissolved organic carbon, i.e., decreasing from 5×10^{-9} to $1 \times 10^{-9} \text{ mM}$ as the organic carbon increased from 1 to 4 mg L^{-1} .

3.4. Degradation intermediates and pathway

The mechanism of 2,6-DMA oxidation by OH^\bullet was also investigated. The concentrations of 2,6-DMA and Fenton's reagent were increased 10 times in order to raise the intermediate concentrations to a level that could be accurately identified by GC/MS and IC. In addition, several extra experiments were also performed using the identified aromatic intermediates (2,6-DMP; 2,6-DMN and 2,6-DMB) as the target compounds to identify their respective oxidation products in order to cross-check the results. The aromatic intermediates found with 80% matching quality or greater were 2,6-DMN, 2,6-DMP, 2,6-DMB, 2,6-dimethyl-hydroquinone (2,6-DMH), 2,6-dimethyl-nitrophenol, and 2,6-dimethyl-3-hydroxybenzoquinone as shown in Table 2. This indicated that the methyl group on the aromatic ring was less sensitive to OH^\bullet attack than amine- and nitro-functional groups. In addition to aromatic intermediates, several carboxylic acids were also detected; including

Table 2
Identified aromatic intermediates of 2,6-DMA oxidation by OH^\bullet .

Retention time (min)	Chemical formula	Q^a (%)
8.000	$\text{C}_8\text{H}_8\text{O}_2$ (2,6-dimethyl-benzoquinone)	83
8.097	$\text{C}_8\text{H}_{10}\text{O}$ (2,6-dimethyl-phenol)	97
8.943	$\text{C}_8\text{H}_9\text{NO}_2$ (2,6-dimethyl-nitrobenzene)	98
9.046	$\text{C}_8\text{H}_8\text{O}_3$ (2,6-dimethyl-3-hydroxy- <i>p</i> -benzoquinone)	80
10.046	$\text{C}_8\text{H}_{10}\text{O}_2$ (2,6-dimethyl-hydroquinone)	81
10.674	$\text{C}_8\text{H}_9\text{NO}_3$ (2,6-dimethyl-nitrophenol)	90

^a Q is the matching quality when compared with the mass spectrum in the Wiley7n database.

maleic, lactic, oxalic, acetic, and formic acids. The pathway of 2,6-DMA oxidation by OH^\bullet is proposed as shown in Fig. 6. The proposed mechanism is quite similar to those of aniline oxidation by either OH^\bullet in Fenton processes [10] and catalytic ozonation [11] or oxygen in wet air oxidation [12]. This is understandable since the methyl group on the aromatic ring of 2,6-DMA was not susceptible to OH^\bullet attack as mentioned previously; therefore, OH^\bullet would attack other sites around the benzene ring (either at amine or hydrogen positions) as if it was AN. In addition, several identified species obtained from this study were also in agreement with Skoumal et al. [13] who studied the oxidation of chloroxylenol by electrochemical advanced oxidation processes. They found OH^\bullet attacked at the chlorine position to form 2,6-DMH, which was further oxidized to 2,6-DMB and several carboxylic acids similar to the observation in this study. Moreover, the ring-cleavage C-3 or lower compounds identified in this work were corresponding very well with the reaction network for the catalytic wet air oxidation of maleic acid proposed by Oliviero et al. [14].

The time profiles of the major products are illustrated in Fig. 7(a), which reveals that the concentrations of the aromatic intermediates were very low (i.e., less than 0.015 mM) even though 80% of 10 mM 2,6-DMA was already transformed.

This indicates that the aromatic ring was rapidly ruptured to form open-chain products. Acetic and formic acids, which are the most successive organic products prior to conversion to CO_2 , were accumulated in the solution. This implies that under the studied conditions within 60 min of reaction time, 2,6-DMA could not be completely mineralized to CO_2 . This is in agreement with the total organic carbon profile as shown in Fig. 7(b) in which only 35% of initial organic carbon could be converted to CO_2 . Considering the carbon balance at the end of the reaction period, it can be seen that approximately 70% of the organic carbon could be quantified from the identified intermediates.

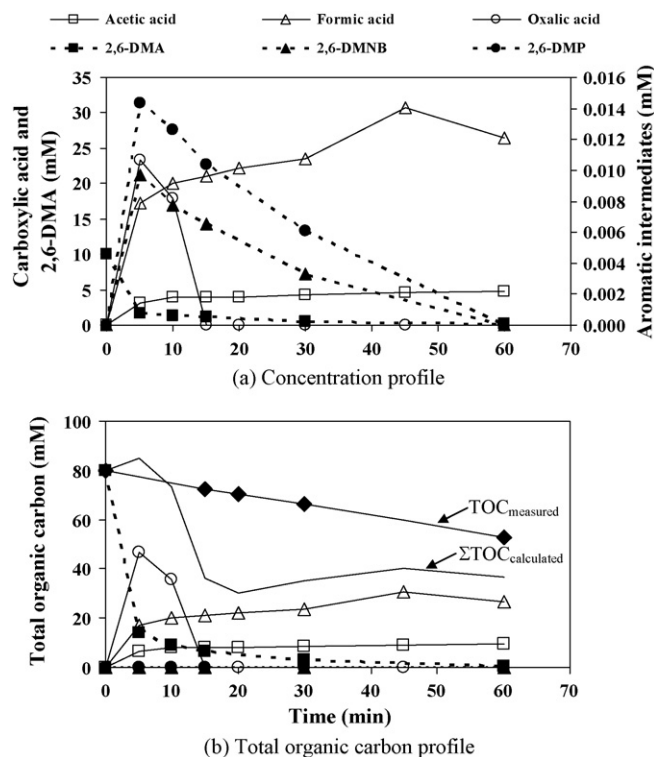


Fig. 7. Intermediate products and TOC profiles of 10 mM 2,6-DMA degradation by Fenton's reaction with 10 mM Fe^{2+} and 200 mM H_2O_2 at pH 3 and 25 °C.

4. Conclusions

This research has determined the intrinsic second-order rate constant for the reaction between 2,6-DMA and OH[•], which has not been previously reported. The rate constants obtained from various conditions under both batch and continuous operations were between 1.59×10^{10} and $1.80 \times 10^{10} \text{ M}^{-1} \text{ s}^{-1}$ with an average of $1.71 \times 10^{10} \text{ M}^{-1} \text{ s}^{-1}$. Identified intermediates included 2,6-dimethyl-nitrobenzene, 2,6-dimethyl-phenol, 2,6-dimethyl-nitrophenol, 2,6-dimethyl-hydroquinone, 2,6-dimethyl-benzoquinone, 2,6-dimethyl-3-hydroxy-benzoquinone, maleic, lactic, oxalic, acetic, and formic acids indicating that the methyl group on the aromatic ring was not susceptible to OH[•] attack. Finally, the degradation pathway of 2,6-DMA by OH[•] oxidation was proposed.

Acknowledgements

This research was financially supported by the Thailand Research Fund through the Royal Golden Jubilee Ph.D. Program (Grant No. PHD/0056/2549), the National Center of Excellence for Environmental and Hazardous Waste Management of Thailand, and the National Science Council of Taiwan (Grant No. NSC96-2628-E-041-001-MY3).

References

- [1] NTP, National Toxicology Program, Toxicology and Carcinogenesis Studies of 2,6-Xylydine (2,6-dimethylaniline) in Charles River CD Rats (Feed Studies), TR 278 U.S. Department of Health and Human Services, Public Health Service, 1990, http://ntp.niehs.nih.gov/ntp/htdocs/LT_rpts/tr278.pdf (accessed April 2009).
- [2] IARC, Monographs on the Evaluation of Carcinogenic Risks to Humans, 57, 1993.
- [3] W.P. Ting, M.C. Lu, Y.H. Huang, Kinetics of 2,6-dimethylaniline degradation by electro-Fenton process, *J. Hazard. Mater.* 161 (2009) 1484–1490.
- [4] J.M. Shen, Z.L. Chen, Z.Z. Xu, X.Y. Li, B.B. Xu, F. Qi, Kinetics and mechanism of degradation of *p*-chloronitrobenzene in water by ozonation, *J. Hazard. Mater.* 152 (2008) 1325–1331.
- [5] APHA, Standard Methods for the Examination of Water and Wastewater, 18th ed., American Public Health Association, Washington, DC, 1992.
- [6] I.M. Kolthof, E.B. Sandell, E.J. Meehan, S. Buckstein, Quantitative chemical analysis, 4th ed., Macmillan, New York, 1969, pp. 1862–1867.
- [7] G.V. Buxton, C.L. Greenstock, W.P. Helman, A.B. Ross, Critical review of rate constants for reactions of hydrated electrons, hydrogen atoms and hydroxyl radicals ([•]OH/[•]O⁻) in aqueous solution, *J. Phys. Chem. Ref. Data* 17 (1988) 513–886.
- [8] M.E. Lindsey, M.A. Tarr, Quantitation of hydroxyl radical during Fenton oxidation following a single addition of iron and peroxide, *Chemosphere* 41 (2000) 409–417.
- [9] J. Hoigne, Chemistry of aqueous ozone and transformation of pollutants by ozonation and advanced oxidation processes, in: O. Hutzinger (Ed.), *Handbook of Environmental Chemistry*, vol. 5, Springer-Verlag, Berlin, 1998, pp. 83–141 (Part C).
- [10] E. Brillas, E. Mur, R. Sauleda, L. Sanchez, J. Peral, X. Domenech, J. Casadi, Aniline mineralization by AOP's: anodic oxidation, photocatalysis, electro-Fenton and photoelectro-Fenton processes, *Appl. Catal. B Environ.* 16 (1) (1998) 31–42.
- [11] R. Sauleda, E. Brillas, Mineralization of aniline and 4-chlorophenol in acidic solution by ozonation catalyzed with Fe²⁺ and UVA light, *Appl. Catal. B Environ.* 29 (2) (2001) 135–145.
- [12] L. Oliviero, H. Wahyu, J. Barbier Jr., D. Duprez, J.W. Ponton, I.S. Metcalfe, D. Mantzavinos, Experimental and predictive approach for determining wet air oxidation reaction pathways in synthetic wastewaters, *Chem. Eng. Res. Des.* 81 (3) (2003) 384–392.
- [13] M. Skoumal, C. Arias, P.L. Cabot, F. Centellas, J.A. Garrido, R.M. Rodriguez, E. Brillas, Mineralization of the biocide chloroxylenol by electrochemical advanced oxidation processes, *Chemosphere* 71 (2008) 1718–1729.
- [14] L. Oliviero, J. Barbier Jr., D. Duprez, H. Wahyu, J.W. Ponton, I.S. Metcalfe, D. Mantzavinos, Wet air oxidation of aqueous solutions of maleic acid over Ru/CeO₂ catalysts, *Appl. Catal. B Environ.* 35 (1) (2001) 1–12.